Bulletin of the Seismological Society of America, Vol. 95, No. 2, pp. 684–698, April 2005, doi: 10.1785/0120040007

Assessing the Quality of Earthquake Catalogues: Estimating the Magnitude of Completeness and Its Uncertainty

by Jochen Woessner and Stefan Wiemer

Abstract We introduce a new method to determine the magnitude of completeness M_c and its uncertainty. Our method models the entire magnitude range (EMR method) consisting of the self-similar complete part of the frequency-magnitude distribution and the incomplete portion, thus providing a comprehensive seismicity model. We compare the EMR method with three existing techniques, finding that EMR shows a superior performance when applied to synthetic test cases or real data from regional and global earthquake catalogues. This method, however, is also the most computationally intensive. Accurate knowledge of M_c is essential for many seismicity-based studies, and particularly for mapping out seismicity parameters such as the *b*-value of the Gutenberg-Richter relationship. By explicitly computing the uncertainties in M_c using a bootstrap approach, we show that uncertainties in *b*-values are larger than traditionally assumed, especially when considering small sample sizes.

As examples, we investigated temporal variations of M_c for the 1992 Landers aftershock sequence and found that it was underestimated on average by 0.2 with former techniques. Mapping M_c on a global scale, M_c reveals considerable spatial variations for the Harvard Centroid Moment Tensor (CMT) ($5.3 \leq M_c \leq 6.0$) and the International Seismological Centre (ISC) catalogue ($4.3 \leq M_c \leq 5.0$).

Introduction

Earthquake catalogues are one of the most important products of seismology. They provide a comprehensive database useful for numerous studies related to seismotectonics, seismicity, earthquake physics, and hazard analysis. A critical issue to be addressed before any scientific analysis is to assess the quality, consistency, and homogeneity of the data. Any earthquake catalogue is the result of signals recorded on a complex, spatially and temporally heterogeneous network of seismometers, and processed by humans using a variety of software and assumptions. Consequently, the resulting seismicity record is far from being calibrated, in the sense of a laboratory physical experiment. Thus, even the best earthquake catalogues are heterogeneous and inconsistent in space and time because of networks' limitations to detect signals, and are likely to show as many man-made changes in reporting as natural ones (Habermann, 1987; Habermann, 1991; Habermann and Creamer, 1994; Zuniga and Wiemer, 1999). Unraveling and understanding this complex fabric is a challenging yet essential task.

In this study, we address one specific aspect of quality control: the assessment of the magnitude of completeness, M_c, which is defined as the lowest magnitude at which 100% of the events in a space–time volume are detected (Rydelek and Sacks, 1989; Taylor *et al.*, 1990; Wiemer and Wyss, 2000). This definition is not strict in a mathematical sense, and is connected to the assumption of a power-law behavior of the larger magnitudes. Below M_c, a fraction of events is missed by the network (1) because they are too small to be recorded on enough stations; (2) because network operators decided that events below a certain threshold are not of interest; or, (3) in case of an aftershock sequence, because they are too small to be detected within the coda of larger events.

We compare methods to estimate M_c based on the assumption that, for a given volume, a simple power-law can approximate the frequency-magnitude distribution (FMD). The FMD describes the relationship between the frequency of occurrence and the magnitude of earthquakes (Ishimoto and Iida, 1939; Gutenberg and Richter, 1944):

$$\log_{10} N(M) = a - bM, \tag{1}$$

where *N(M)* refers to the frequency of earthquakes with magnitudes larger or equal than *M*. The *b*-value describes the relative size distribution of events. To estimate the *b*-value, a maximum-likelihood technique is the most appropriate measure:

$$b = \frac{\log_{10}(e)}{\left[\langle M \rangle - \left(M_c - \Delta M_{\text{bin}}/2\right)\right]}. \tag{2}$$

Here $\langle M \rangle$ is the mean magnitude of the sample and ΔM_{bin} is the binning width of the catalogue (Aki, 1965; Bender, 1983; Utsu, 1999).

Rydelek and Sacks (2003) criticized Wiemer and Wyss (2000), who had performed detailed mapping of M_c, for using the assumption of earthquake self-similarity in their methods. However, Wiemer and Wyss (2003) maintain that the assumption of self-similarity is in most cases well founded, and that breaks in earthquake scaling claimed by Rydelek and Sacks (2003) are indeed caused by temporal and spatial heterogeneity in M_c. The assumption that seismic events are self-similar for the entire range of observable events is supported by studies of, for example, von Seggern *et al.* (2003) and Ide and Beroza (2001).

A "safe" way to deal with the dependence of *b*- and *a*-values on M_c is to choose a large value of M_c, but this seems overly conservative. However, this approach decreases the amount of available data, reducing spatial and temporal resolution and increasing uncertainties due to smaller sample sizes. Maximizing data availability while avoiding bias due to underestimated M_c is desirable; moreover, it is essential when one is interested in questions such as studying breaks in magnitude scaling (Abercrombie and Brune, 1994; Knopoff, 2000; Taylor *et al.*, 1990; von Seggern *et al.*, 2003). Unless the space–time history of $M_c = M_c(x,y,z,t)$ is taken into consideration, a study would have to conservatively assume the highest M_c observed. It is further complicated by the need to determine M_c automatically, since in most applications, numerous determinations of M_c are needed when mapping parameters such as seismicity rates or *b*-values (Wiemer and Wyss, 2000; Wiemer, 2001).

A reliable M_c determination is vital for numerous seismicity- and hazard-related studies. Transients in seismicity rates, for example, have increasingly been scrutinized, as they are closely linked to changes in stress or strain, such as static and dynamic triggering phenomena (e.g., Gomberg *et al.*, 2001; Stein, 1999). Other examples of studies that are sensitive to M_c are scaling-related investigations (Knopoff, 2000; Main, 2000) or aftershock sequences (Enescu and Ito, 2002; Woessner *et al.*, 2004). In our own work on seismic quiescence (Wiemer and Wyss, 1994; Wyss and Wiemer, 2000), *b*-value mapping (Wiemer and Wyss, 2002; Gerstenberger *et al.*, 2001), and time-dependent hazard (Wiemer, 2000), for example, we often found M_c to be the most critical parameter of the analysis. Knowledge of $M_c(x,y,z,t)$ is important, because a minute change in M_c in $\Delta M_c = 0.1$ leads (assuming $b = 1.0$) to a 25% change in seismicity rates; a change of $\Delta M_c = 0.3$ reduces the rate by a factor of two.

The requirements for an algorithm to determine M_c in our assessment are: (1) to calculate M_c automatically for a variety of datasets; (2) to give reliable uncertainty estimates; and (3) to conserve computer time. We specifically limit our study to techniques based on parametric data of modern earthquake catalogues. A number of researchers have investigated detection capability by studying signal-to-noise ratios at particular stations (Gomberg, 1991; Kvaerna *et al.*, 2002a,b); however, these waveform-based techniques are generally too time-consuming to be practical for most studies. We also focus on recent instrumental catalogues, ignoring the question of how to best determine M_c in historical datasets commonly used in seismic hazard assessment (Albarello *et al.*, 2001; Faeh *et al.*, 2003). In order to evaluate the performance of the different algorithms, we use synthetically-created regional and global data sets.

We believe that the review and comparison of adaptable methods presented in this article, and the introduction of uncertainties in M_c, are an important contribution for improving seismicity related studies.

Data

For the comparison of methods to determine M_c, we chose subsets of six different catalogues with diverse properties. The catalogues analyzed are freely available from the websites of the specific agencies:

- Regional catalogue: We selected a subset of the Earthquake Catalogue of Switzerland (ECOS) of the Swiss Seismological Service (SSS) in the southern province Wallis for the period 1992–2002 (Fig. 1A), providing a local magnitude M_L (Deichmann *et al.*, 2002).
- Regional catalogue: We chose a subset of the Northern California Seismic Network (NCSN) catalogue focused on the San Francisco Bay area for the period 1998–2002, using the preferred magnitude (Fig. 1B).
- Volcanic region: We use a subset of the earthquake catalogue maintained by the National Research Institute for Earth Science and Disaster Prevention (NIED) reporting a local magnitude M_L. The subset spans a small volcanic region in the Kanto province for the period 1992–2002 (Fig. 1C).
- Aftershock sequence: We selected a seven year period (1992–1999) from the Landers 1992 M_W 7.3 aftershock sequence, using the earthquakes recorded by the Southern California Seismic Network (SCSN), a cooperative project of Caltech and the U.S. Geological Survey, distributed through the Southern California Earthquake Data Center (SCEDC), reporting a local magnitude M_L (Fig. 1D).
- Global datasets:
  a. the Harvard Centroid Moment Tensor (CMT) catalogue, reporting the moment magnitude M_W, is used for the time period 1983–2002. Only shallow events ($d \leq 70$km) are used for mapping purposes.
  b. the International Seismological Centre (ISC) catalogue is analyzed for the period 1980–2000 and magnitudes $m_b \geq 4.3$. Only shallow events ($d \leq 70$km) are used. The cut-off magnitude was chosen due to the temporal heterogeneity of the catalogue. Surface wave magnitudes are taken to equal m_b in case there is none.

From this point on, we refer to the generic expression

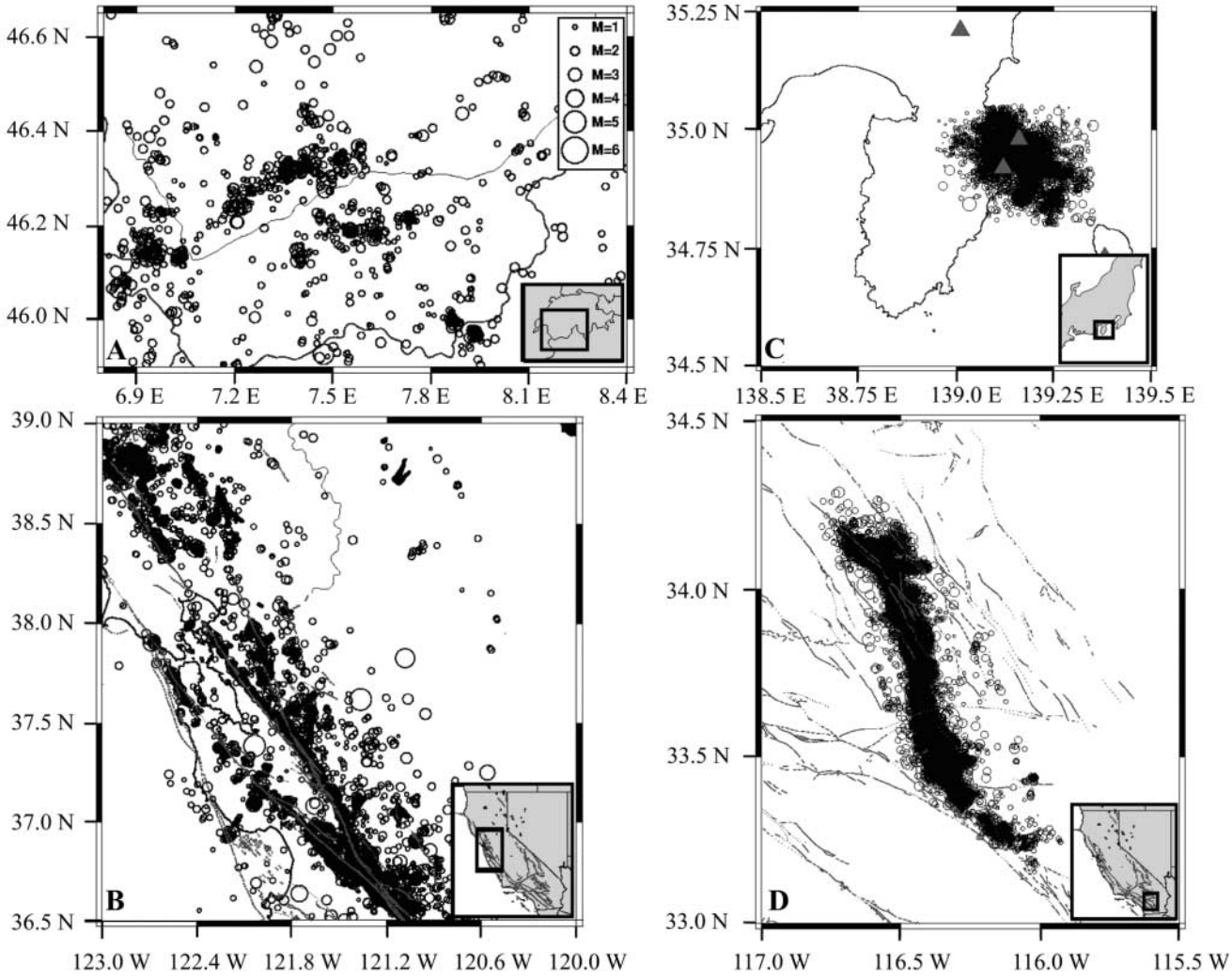

Figure 1. Earthquakes used in this study: (A) Subset of the earthquake catalogue of Switzerland (ECOS) in the southern province Wallis; (B) subset of the NCSN catalogue comprising the San Francisco Bay area; (C) subset of the NIED catalogue in the Kanto province with the triangles indicating volcanoes; and (D) the Landers 1992 aftershock sequence from the SCSN catalogue. California maps display known faults in light gray.

"magnitude" that corresponds to the magnitude of the respective earthquake catalogue outlined above.

Methods

Methods to estimate the magnitude of completeness of earthquake catalogues are based on two fundamentally different assumptions. Most methods assume self-similarity of the earthquake process, which consequently implies a power-law distribution of earthquakes in the magnitude and in the seismic moment domain. One other approach relies on the assumption that the detection threshold due to noise decreases at night, thus the magnitude of completeness is determined using the day-to-night ratio of earthquake frequency (Rydelek and Sacks, 1989; Taylor *et al.*, 1990). In this study, we compare only methods assuming self-similarity of the earthquake process:

1. Entire-magnitude-range method (EMR) modified from Ogata and Katsura (1993)
2. Maximum curvature-method (MAXC) (Wiemer and Wyss, 2000)
3. Goodness-of-fit test (GFT) (Wiemer and Wyss, 2000)
4. M_c by *b*-value stability (MBS) (Cao and Gao, 2002)

These methods are described below and are illustrated schematically in Figure 2. The code is freely available together with the seismicity analysis software package ZMAP (Wiemer, 2001), which is written in Mathworks' commercial software language Matlab® (http://www.mathworks.com).

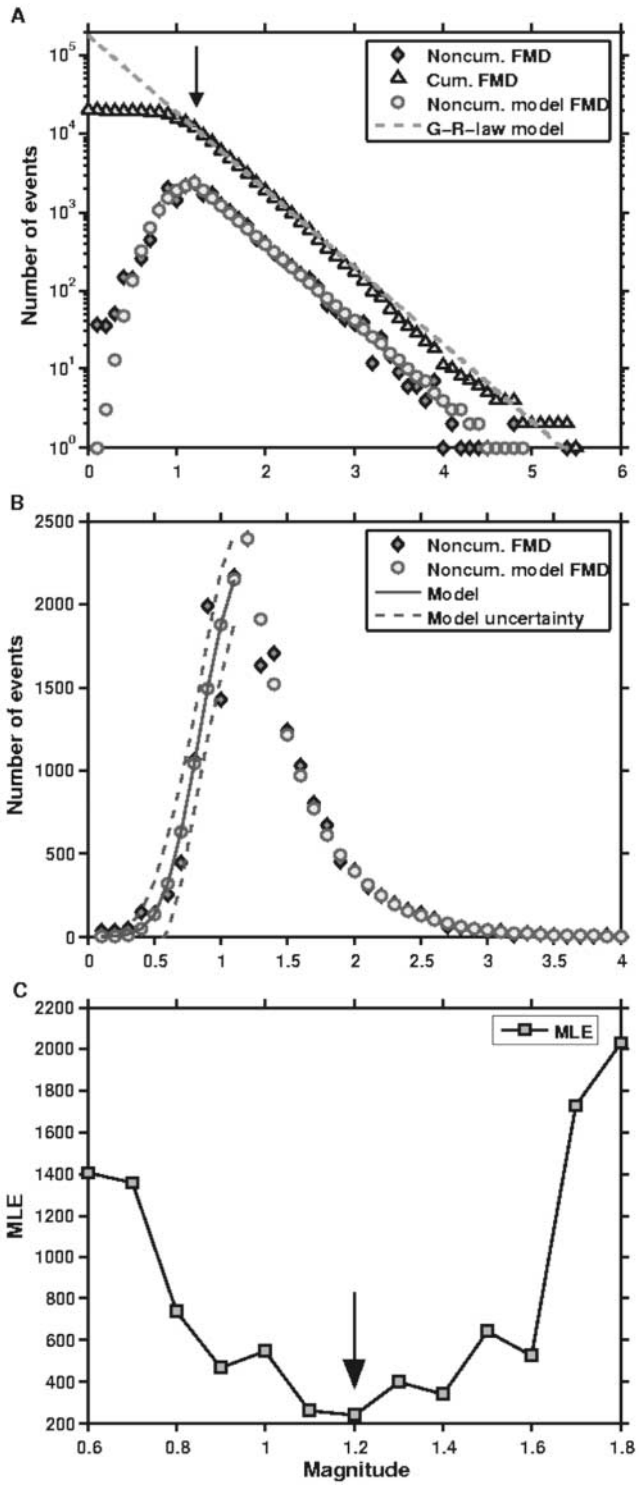

Figure 2. EMR method applied to the NCSN-catalogue data (1998–2001): $M_c = 1.2$, $b = 0.98$, $a = 5.25$, $\mu = 0.73$, $\sigma = 21$. (A) Cumulative and non-cumulative FMD and model on logarithmic scale with the arrow indicating M_c. (B) Normal CDF fit (gray line) to the data below $M_c = 1.2$ on linear scale. Standard deviations of the model, dashed gray line; original data, diamonds; non-cumulative FMD of EMR-model, circles. (C) Choice of the best model from the maximum-likelihood estimates denoted with an arrow pointing to the resulting M_c-value.

EMR Method

We developed a method to estimate M_c that uses the entire data set, including the range of magnitudes reported incompletely. Our approach is similar to that of Ogata and Katsura (1993), and uses a maximum-likelihood estimator for a model that consists of two parts: one to model the complete part, and one to sample the incomplete part of the frequency-magnitude distribution (Fig. 2). We use the entire magnitude range to obtain a more robust estimate of M_c, especially for mapping purposes.

For data above an assumed M_c, we presume a power-law behavior. We compute a- and b-values using a maximum-likelihood estimate for the a- and b-value (Aki, 1965; Utsu, 1965). For data below the assumed M_c, a normal cumulative distribution function $q(M|\mu,\sigma)$ that describes the detection capability as a function of magnitude is fitted to the data. $q(M|\mu,\sigma)$ denotes the probability of a seismic network to detect an earthquake of a certain magnitude and can be written as:

$$q(M|\mu,\sigma) = \begin{cases} \dfrac{1}{\sigma\sqrt{2\pi}} \displaystyle\int_{-\infty}^{M_c} \exp\left(-\frac{(M-\mu)^2}{2\sigma^2}\right) dM, & M < M_c \\ 1, & M \geq M_c. \end{cases} \quad (3)$$

Here, μ is the magnitude at which 50% of the earthquakes are detected and σ denotes the standard deviation describing the width of the range where earthquakes are partially detected. Higher values of σ indicate that the detection capability of a specific network decreases faster. Earthquakes with magnitudes equal to or greater than M_c are assumed to be detected with a probability of one. The free parameters μ and σ are estimated using a maximum-likelihood estimate.

The best fitting model is the one that maximizes the log-likelihood function for four parameters: μ and σ, as well as a and b. As the negative log-likelihoods are computed, we changed the sign for display reasons so that the minimum actually shows the maximum likelihood estimate in Figure 2C. The circles in Figure 2B show the best fit for the dataset in Figure 2A.

We tested four functions to fit the incomplete part of real earthquake catalogues: three cumulative distribution functions (exponential, lognormal, and normal) and an exponential decay. The latter two cumulative distribution functions (CDF) are competitive when computing the likelihood score. However, the normal CDF generally best fits the data from regional to worldwide earthquake catalogues compared to the other functions.

The EMR method creates a comprehensive seismicity model. To evaluate if this model is acceptable compared to the actual data, we adopt a Kolmogorov-Smirnov test (KS test) at the 0.05 significance level to examine the goodness-of-fit (Conover, 1999). The test assumes that the two samples are random and mutually independent. The null hy-

pothesis H_0 of the test is that the two samples are drawn from the same distribution.

Maximum Curvature (MAXC)

Wiemer and Wyss (2000) proposed two methods based on the assumption of self-similarity. A fast and reliable estimate of M_c is to define the point of the maximum curvature (MAXC) as magnitude of completeness by computing the maximum value of the first derivative of the frequency-magnitude curve. In practice, this matches the magnitude bin with the highest frequency of events in the non-cumulative frequency-magnitude distribution, as indicated in Figure 3A. Despite the easy applicability and relative robustness of this approach, M_c is often underestimated especially for gradually-curved frequency-magnitude distributions that result from spatial or temporal heterogeneities.

Goodness-of-Fit test (GFT)

The GFT-method to calculate M_c compares the observed frequency-magnitude distribution with synthetic ones (Wiemer and Wyss, 2000). The goodness-of-fit is computed as the absolute difference of the number of events in the magnitude bins between the observed and synthetic Gutenberg-Richter distribution. Synthetic distributions are calculated using estimated *a*- and *b*-values of the observed dataset for $M \geq M_{co}$ as a function of ascending cutoff magnitudes M_{co}. *R* defines the fit in percentage to the observed frequency-magnitude distribution, and is computed as a function of

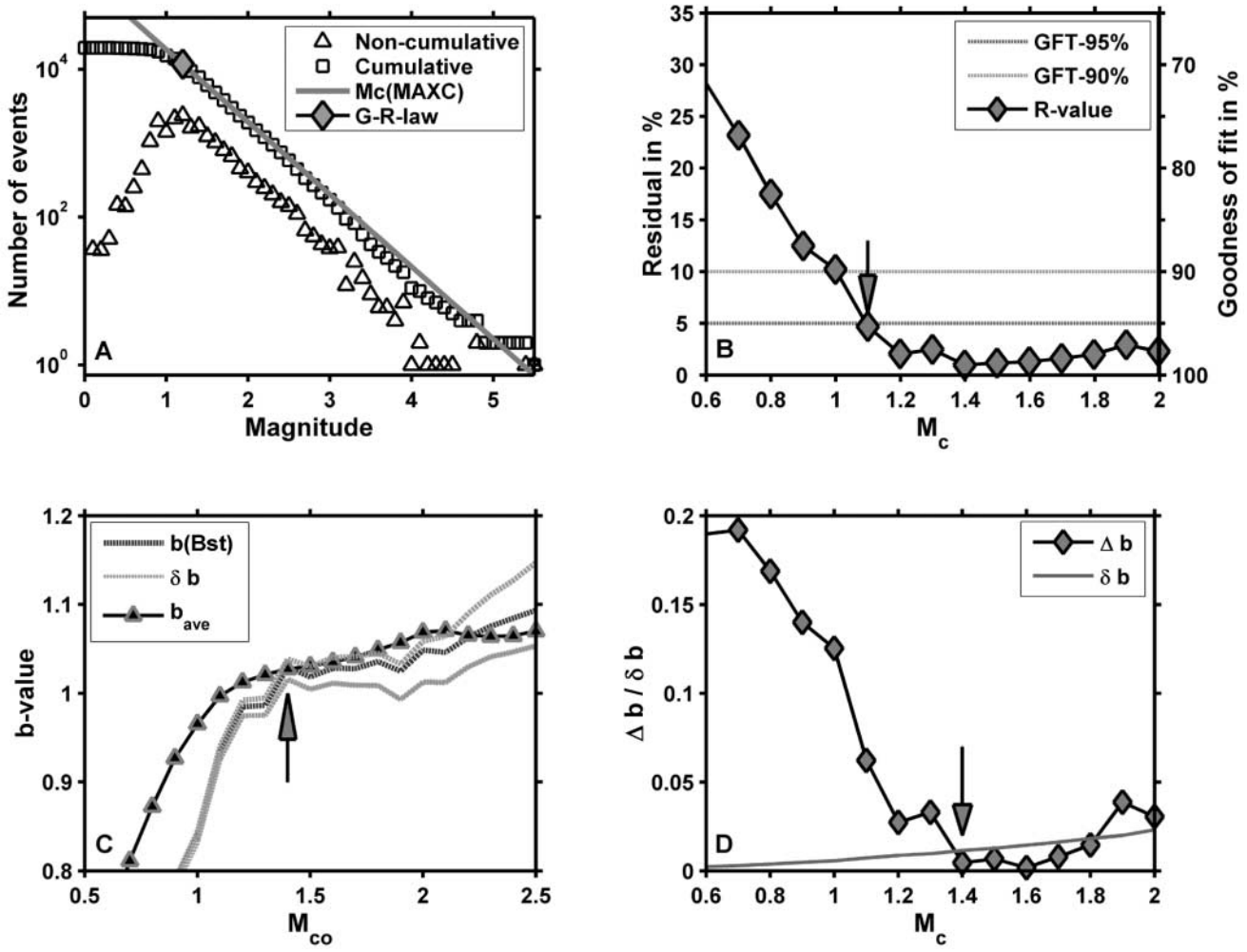

Figure 3. (A) Frequency-magnitude distribution of the subset of the NCSN catalogue. The result of the MAXC approach is indicated with a diamond. (B) Residuals and goodness-of-fit value *R* for the GFT-method. *R* is the difference between the observed and synthetic FMDs, as a function of M_c. Dashed horizontal lines indicate at which magnitudes 90% and 95% of the observed data are modeled by a straight line fit. (C) *b*, b_{ave} and the uncertainties δb as a function of cutoff magnitude M_{co} for the MBS approach. The decision criterion is displayed in panel D. (D) Standard deviation δb and difference $\Delta b = |b - b_{ave}|$ as a function of M_{co}. M_c is defined at the cutoff magnitude for which $\Delta b \leq \delta b$ for the first time.

cutoff magnitude. A model is found at an *R*-value at which a predefined percentage (90% or 95%) of the observed data is modeled by a straight line. Figure 3B shows a schematic example with the choice of M_c indicated by the arrow as the *R*-value falls below the horizontal line of the 95% fit. Note that it is not the minimum *R*-value that is chosen. The 95% level of fit is rarely obtained for real catalogues; the 90% level is a compromise.

M_c by *b*-value Stability (MBS)

Cao and Gao (2002) estimate M_c using the stability of the *b*-value as a function of cutoff magnitude M_{co}. This model is based on the assumption that *b*-values ascend for $M_{co} < M_c$, remain constant for $M_{co} \geq M_c$, and ascend again for $M_{co} \gg M_c$. If $M_{co} \ll M_c$, the resulting *b*-value will be too low. As M_{co} approaches M_c, the *b*-value approaches its true value and remains constant for $M_{co} \gg M_c$, forming a plateau (Fig. 3C). These authors arbitrarily defined M_c as the magnitude for which the change in *b*-value, $\Delta b(M_{co})$ of two successive M_{co}, is smaller than 0.03. Testing this approach for mapping purposes, we found the criterion to be unstable, since the frequency of events in single magnitude bins can vary strongly. To base the approach on an objective measure and to stabilize it numerically, we decided to use the *b*-value uncertainty according to Shi and Bolt (1982) as criterion:

$$\delta b = 2.3b^2 \sqrt{\frac{\sum_{i=1}^{N} (M_i - \langle M \rangle)}{N(N-1)}}, \qquad (4)$$

with $\langle M \rangle$ being the mean magnitude and *N* the number of events.

We define M_c as the magnitude at which $\Delta b = |b_{ave} - b| \leq \delta b$ (Fig. 3D). The arithmetic mean, b_{ave}, is calculated from *b*-values of successive cutoff magnitudes in half a magnitude range $dM = 0.5$: $b_{ave} = \sum_{M_{co}=1.5}^{2} b(M_{co}) \,/\, 5$ for a bin size of 0.1. Note that the magnitude range dM to calculate b_{ave} is crucial. If one chose, for example, $dM = 0.3$, the resulting M_c can be very different from the one obtained using $dM = 0.5$. Large magnitude ranges are preferable, and would be justified for frequency-magnitude distributions that perfectly obey a power-law. Figure 3C shows *b,* b_{ave} and δb as a function of M_{co}. At $M_{co} = 1.4$, b_{ave} is within the uncertainty bounds δb (Fig. 3D), thus $M_c = 1.4$.

Additional Methods

Several other authors proposed additional methods to estimate the magnitude of completeness. Some of these methods are rather similar to the ones outlined above; one method is based on other assumptions. For the reasons described in the following, we did not add these methods to our comparison.

Kagan (2003) proposed a method for fitting the empirical distribution of the observed data with the Pareto-law in the seismic moment domain using fixed β-values. The goodness-of-fit is computed applying a KS test. This approach is similar in concept to the GFT method, but applies a rigorous statistical test. However, we found this method to show instabilities when using a grid search technique to simultaneously fit *b* and M_c.

Marsan (2003) introduced a method computing the *b*-value and the log-likelihood of completeness for earthquakes above a certain cutoff magnitude. The log-likelihood of completeness is defined as the logarithmic probability that the Gutenberg-Richter law fitted to the data above the cutoff magnitude can predict the number of earthquakes in the magnitude bin just below the cutoff magnitude. The magnitude of completeness is chosen so that (1) the *b*-value drops for magnitudes smaller than M_c, and (2) the log-likelihood drops at M_c. The method is similar to the MBS method, but the two criteria are difficult to combine for automatic M_c calculations. Additionally, calculating the log-likelihood for only one magnitude bin bears instabilities, as the frequencies of events in the magnitude bins varies strongly.

Rydelek and Sacks (1989) introduced a method to estimate M_c using a random walk simulation (Schuster's method). The test assumes (1) that earthquakes, at any magnitude level, follow a Poisson distribution; and (2) that due to higher, man-made noise-levels during daytime, M_c is higher at this time. The method requires that other non-random features in earthquake catalogues, such as swarms, aftershock sequences, or mine blasts, are removed in advance, implying that it is not useful for the determination of M_c if such features are present, and thereby placing strong limitations on the applicability (Wiemer and Wyss, 2003). In contrast to others, this method does not assume self-similarity of earthquakes, which is the main reason not to include it in the comparison, as we want to compare methods based on the same assumption.

Estimating the Uncertainty of M_c and *b*

None of the aforementioned methods has yet explicitly considered the uncertainty in the estimate of M_c and its influence on the *b*-value. We use a Monte Carlo approximation of the bootstrap method (Efron, 1979; Chernick, 1999) to calculate the uncertainties δM_c and δb. This can be combined with all methods described in detail. Bootstrap sample earthquake catalogues are generated by drawing with replacement an equivalent amount of events from the original catalogue. For each of the bootstrap sample earthquake catalogues, M_c and *b* are calculated. The second moment of the evolving empirical distributions of M_c and *b*-values is defined as the uncertainty δM_c and δb, respectively.

Note that we use the mean values of the empirical distributions for M_c and *b* as final results for automated mapping, not the ones from the single observed frequency-

magnitude distribution. The bootstrap accounts for outliers and, consequently, smoothes the results spatially, which is desirable for mapping purposes. When analyzing the FMD of single subvolumes, one might use the results of the observed frequency-magnitude distribution. In general, bootstrapping itself was designed to estimate the accuracy of a statistic and not to produce a better point estimate, although there are a few exceptions to the rule (Chernick, 1999). However, we choose the mean value, since the mean estimate considers aleatory uncertainties of the magnitude determination process. This implies that the frequency-magnitude distribution of a parametric earthquake catalogue is considered to be the best guess. We do not observe a significant bias of the estimated parameters to either higher or lower values computing the mean values for different types of earthquake catalogues.

Results

Sensitivity of the EMR Method

To quantify the sensitivity of the EMR method to magnitude distributions that do not conform to the assumed normal CDF, we designed synthetic catalogues that follow probabilities of the normal CDF and of two other cumulative distribution functions for magnitudes smaller than the magnitude of completeness: the Weibull and the lognormal CDF. All three distributions have the same number of free parameters. Magnitudes above M_c 1.5 follow a Gutenberg-Richter law with $b = 1$.

For each of the three CDFs, a thousand possible synthetic distributions of magnitudes below M_c are computed, randomly varying the governing parameters of the CDFs. These parameters are constrained so that the probability of detecting events above $M_c \geq 1.5$ is close or equal to 1. For each of these catalogues, we apply the EMR method to obtain M_c and the KS test acceptance indicator H (Fig. 4).

The result shows peaked distributions of M_c, with a small second moments $\delta M_c = 0.006$, $\delta M_c = 0.025$ and $\delta M_c = 0.040$ for the normal, lognormal, and the Weibull CDF, respectively. The KS test results reveal that the seismicity model is accepted 100% for the normal CDF, 94.6% for the lognormal and 84.6% for the Weibull CDF. Thus, the EMR method based on the normal CDF creates a magnitude distribution that resembles the original distribution and results in a good fit, even though the magnitude distribution violates a basic assumption.

Comparing the Methods: Dependence on the Sample Size

We first analyze the dependence of M_c on the sample size S (i.e., number of events), for the different methods. A synthetic catalogue with $M_c = 1$ and $b = 1$ is used: the incomplete part below M_c was modeled using a normal CDF q, with $\mu = 0.5$ and $\sigma = 0.25$. From the synthetic dataset, random samples of ascending size $20 \leq S \leq 1500$ are drawn, and M_c as well as b are computed. For each sample size, this procedure is repeated for $N = 1000$ bootstrap samples.

In general, we expect from each approach to recover the predefined M_c 1.0 and the uncertainties δM_c to decrease with an increasing amount of data. The EMR method is well capable of recovering $M_c = 1.0$ (Fig. 5A). The MBS-approach underestimates M_c substantially for small sample sizes ($S \leq 250$), and shows the strongest dependence on sample size (Fig. 5B). Both the MAXC and GFT-95% − approaches (Figs. 5C and D) underestimate M_c by about 0.1, with MAXC consistently calculating the smallest value. Apart from the MBS approach, δM_c shows the expected decrease with increasing sample size S. Uncertainties of the EMR approach decrease slightly for $S \leq 100$, probably due to the limited data set. The uncertainties of δM_c vary between 0.2 and 0.04, and are smaller for the MAXC approach—on average, almost half the size of the uncertainties computed for the GFT-95% and EMR uncertainties. In case of the MBS approach, the increasing number of samples result in a decrease of the uncertainty δb calculated using equation (4) (Shi and Bolt, 1982). Consequently, the criterion $\Delta b = |b_{ave} - b| \leq \delta b$ becomes stricter and in turn results in higher uncertainties for the M_c determination.

We infer that reliable estimates for M_c can only be obtained for larger sample sizes. However, M_c estimates of the MAXC and EMR approaches result in reasonable values that could be used in case of small datasets. From our investigations, we assume that $S \geq 200$ events are desirable as a minimum sample size S. We are aware of the fact that it is not always possible to achieve this amount when spatially and temporally mapping M_c. For smaller quantities, we suggest further statistical tests for the significance of the results, such as when addressing b-value anomalies (Schorlemmer *et al.*, 2003).

We also addressed the question of how many bootstrap samples are needed to obtain reliable estimates of uncertainties. While Chernick (1999) proposes $N = 100$ bootstrap samples as adequate to establish standard deviations but recommends to use $N = 1000$ depending on available computing power, we find that our results stabilize above $N = 200$.

Comparing the Methods: Real Catalogues

We apply the bootstrap approach to compare the performance of the different methods for a variety of earthquake catalogues. For the comparison, M_c and b-values are calculated simultaneously for $N = 500$ bootstrap samples. Figure 6 illustrates the results in two panels for catalogues of the SSS (A, B), the NCSN (C, D), the NIED (E, F), and the Harvard CMT catalogue (G, H): For each catalogue, b-value versus M_c plots are shown, with each marker indicating the mean values for M_c and b as well as the uncertainties δM_c and δb displayed as error bars. The additional panels show

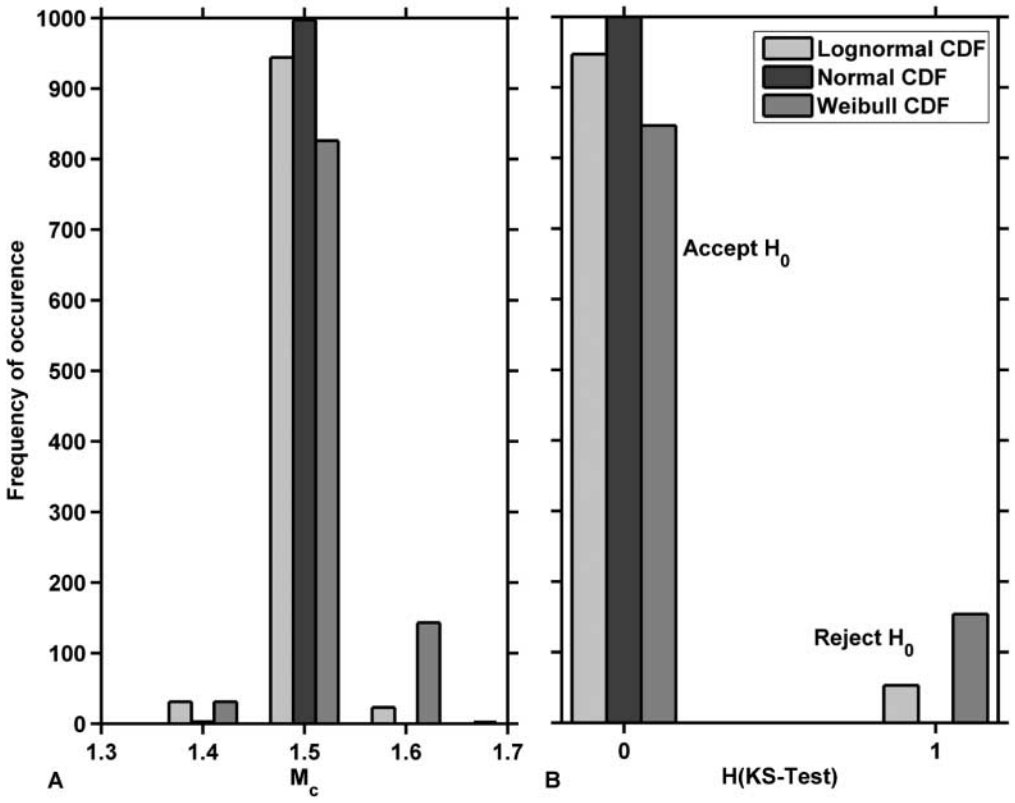

Figure 4. Histograms of (A) M_c-distributions and (B) KS-test acceptance indicator H for synthetic frequency-magnitude distributions randomly created using normal, lognormal and the Weibull CDFs below M_c. Second moments are small and the fractions of accepted models are high in all three cases. In detail, the second moments are $\delta M_c = 0.006$, $\delta M_c = 0.025$, and $\delta M_c = 0.040$; and the fractions of accepted models are 100%, 94.6%, and 84.6% for the normal, lognormal and the Weibull CDF, respectively.

the cumulative and non-cumulative frequency-magnitude distributions of the catalogue. Table 1 summarizes the results.

The comparison exhibits a consistent picture across the different data sets, which also agrees with the results obtained in Figure 4 for the synthetic distribution. However, in contrast to the synthetic distribution, we do not know the true value of M_c in these cases; thus we render a relative evaluation on the performance of the algorithms. While uncertainties across the methods are in the same order of magnitude for both δb and δM_c, respectively, the individual estimates of M_c and b are not consistent. The MBS method leads to the highest M_c values, whereas the MAXC and the GFT-90% approaches appear at the lower limit of M_c. The EMR approach shows medium estimates of both parameters, while estimates of the GFT-95% approach vary strongest. In case of the Harvard CMT catalogue, the GFT-95% approach does not show a result, since this level of fit is not obtained. The MBS approach applied to the NIED and Harvard-CMT catalogues finds $M_c = 1.96$ and $M_c = 6.0$, respectively—much higher than the average values of $M_c \approx 1.2$ and $M_c \approx 5.35$ determined by the other methods. This results from the fact that b as a function of magnitude does not show a plateau region as expected in theory (compare to Fig. 2C).

Case Studies

M_c and b as a Function of Time: The Landers Aftershock Sequence

M_c and b-values vary in space and time. Aftershock sequences provide excellent opportunities to study the behavior of the M_c determination algorithms in an environment of rapid M_c changes (Wiemer and Katsumata, 1999). A reliable estimate of the magnitude of completeness in aftershock sequences is essential for a variety of applications, such as aftershocks hazard assessment, determining modified Omori-law parameters, and detecting rate changes. We investigate the aftershock sequence of the 28, June 1992 M_w 7.3 Landers earthquake, consisting of more than 43,500 events in the seven years following the mainshock ($M_L \geq 0.1$). We selected data in a polygon with a northwest–southeast extension of about 120 km, and a lateral extension of up to 15 km on each side of the fault line. This sequence was investigated by Wiemer and Katsumata (1999), Liu *et al.* (2003), and Ogata *et al.* (2003); however, uncertainties and temporal variations have yet not been taken into account.

We reevaluate the temporal evolution of M_c for the entire sequence, the northernmost and southernmost 20 km of

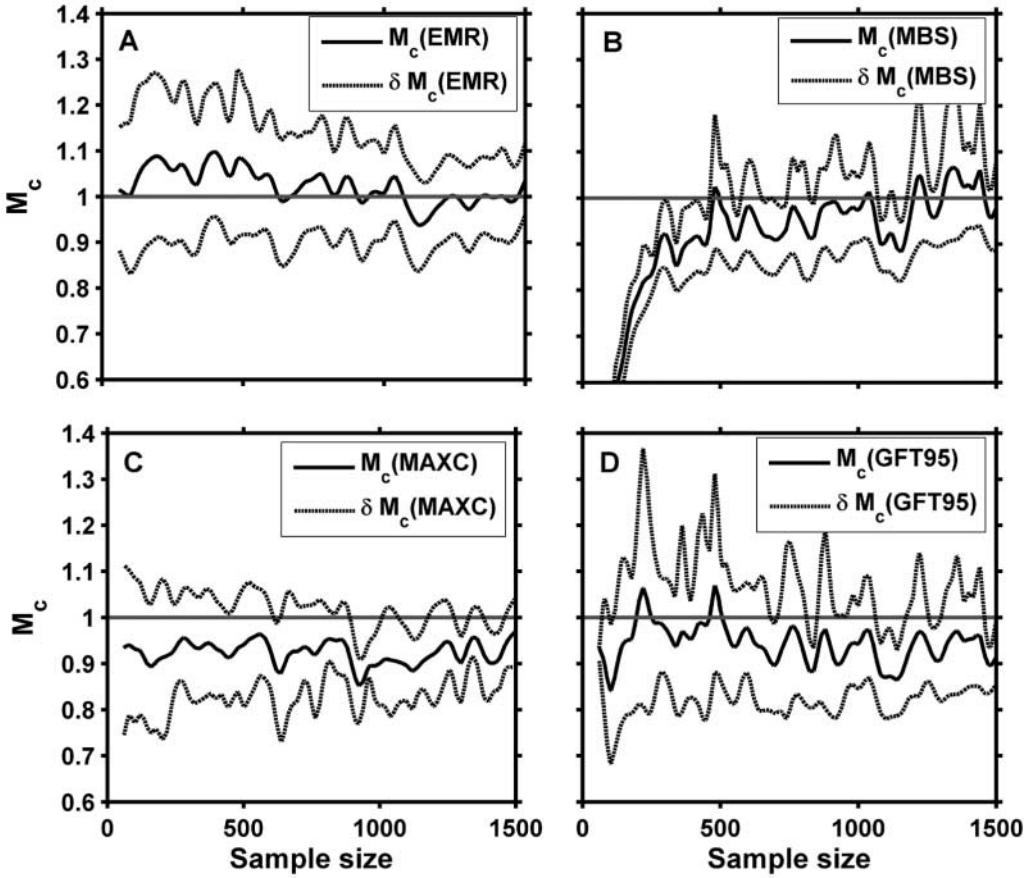

Figure 5. M_c as function of the sample size used for the determination of M_c for a synthetic catalogue. The synthetic catalogue was created with $M_c = 1$, $b = 1$, $\mu = 0.5$, and $\sigma = 0.25$ for the normal CDF. Each subplot displays the mean M_c-values and the uncertainty $M_c \pm \delta M_c$ for (A) the EMR approach, (B) the MBS approach, (C) the MAXC approach, and (D) the GFT-95% method. Note that the uncertainties decrease with increasing sample size for all methods except for the MBS approach.

the Landers rupture. To create the time series, we chose a moving window approach, with a window size of $S = 1000$ events to compute parameters while moving the window by 250 events for the entire sequence. For the subregions, we used $S = 400$ and shifted the window by hundred events. We also analyzed the entire sequence for smaller sample sizes of $S = 400$, which showed slightly higher estimates of M_c, particularly right after the mainshock, but well within the uncertainty bounds of using $S = 1000$ samples.

M_c(EMR) and its uncertainty values are plotted as light gray lines in the background (Fig. 7). Disregarding the first four days, values for the entire sequence (Fig. 7A) vary around $M_c(\text{EMR}) = 1.61 \pm 0.1$, and $M_c(\text{MAXC}) = 1.52 \pm 0.07$; values in the northern part vary around $M_c(\text{EMR}) = 1.84 \pm 0.135$ compared to $M_c(\text{MAXC}) = 1.71 \pm 0.09$ (Fig. 7B). In the southern part (Fig. 7C), values vary around $M_c(\text{EMR}) = 1.54 \pm 0.15$, and $M_c(\text{MAXC}) = 1.37 \pm 0.10$. The comparison reveals that M_c-values are largest in the northern part of the rupture zone and smallest in the south. The MAXC approach used in Wiemer and Katsumata (1999) underestimated M_c on average by 0.2.

Globally Mapping M_c

On a global scale, we apply the EMR method to the Harvard CMT and the MAXC method to the ISC catalogue (Fig. 8). Kagan (2003) analyzed properties of global earthquake catalogues and concluded that the Harvard CMT catalogue is "reasonably complete" for the period 1977–2001, with a magnitude threshold changing between M_w 5.7 before 1983 to about M_w 5.4 in recent years. He analyzed variations of M_c as a function of earthquake depth, tectonic provinces, and focal mechanisms. We exclude the early years before 1983, as those years show a higher M_c and significantly fewer earthquakes (Dziewonski *et al.*, 1999; Kagan, 2003). We apply the EMR approach to map M_c for the Harvard CMT. In case of the more heterogeneous ISC catalogue, we cut the catalogue at $M \geq 4.3$ and apply the MAXC approach. This is necessary because the ISC includes reports from regional networks, and we seek to evaluate the completeness of the catalogue comparable to the Harvard CMT catalogue. We do not consider different focal mechanisms, and limit our study to seismicity in the depth range $d \leq 70$ km. The

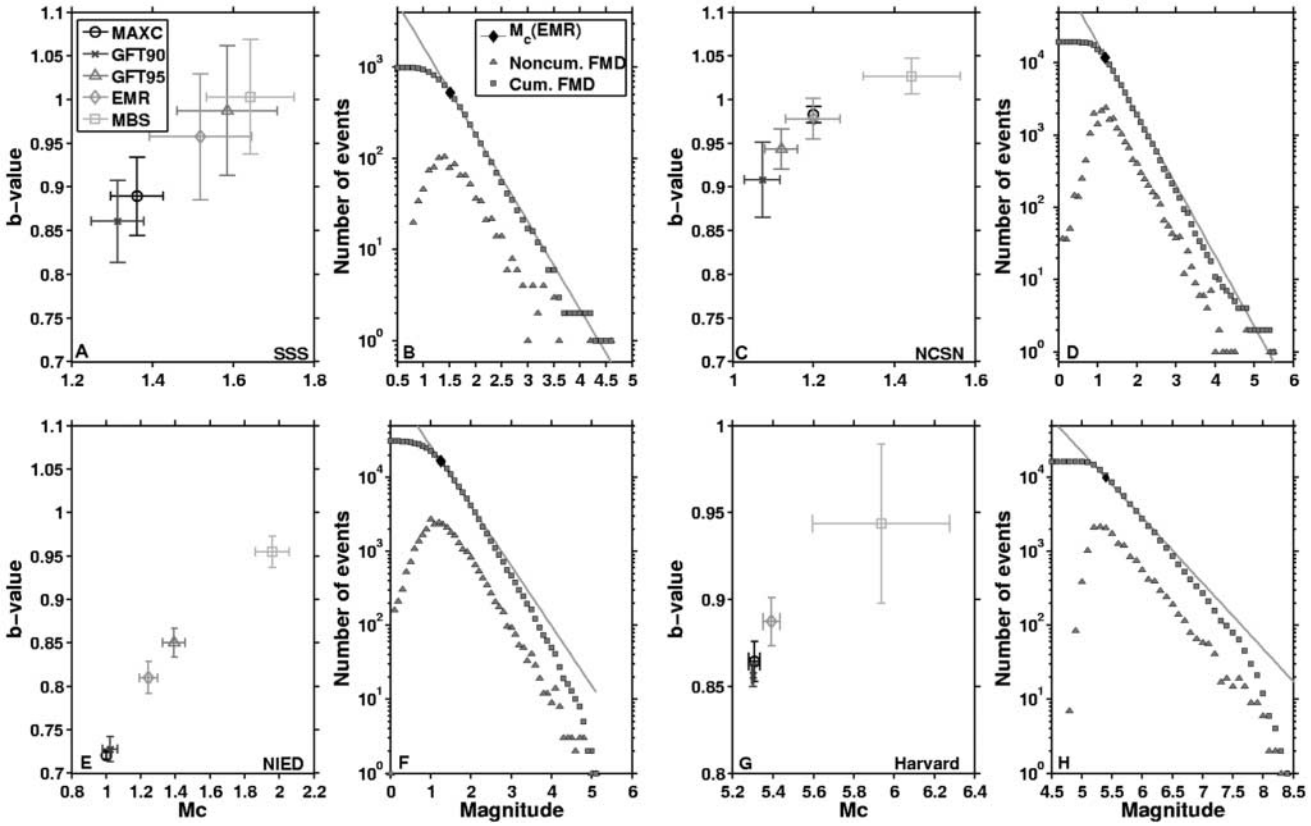

Figure 6. M_c and b-values combined with bootstrap uncertainties indicated as error bars and the corresponding FMDs of four catalogues: (1) regional catalogue: subset of the ECOS catalogue of the SSS in the Wallis province of Switzerland (A, B); (2) regional catalogue: subset of the NCSN catalogue in the San Francisco Bay area (C, D); (3) volcanic area in the Kanto province taken from the NIED catalogue (E, F); (4) global catalogue: results using the Harvard CMT catalogue, no M_c(GFT-95%) determined (G, H). Comparing the results in all panels, MAXC and GFT-90% tend to small, MBS to high, and EMR to medium M_c values. Results from the GFT-95% method reveal no clear tendency. Results are listed in Table 1.

Table 1

Number of Events, Polygons of the Data Sets, M_c and b-values Together with Their Uncertainties Determined for the Data Used in Figure 6

Catalogue	SSS*	NCSN†	NIED‡	Harvard CMT§
Number of events	988	19559	30882	16385
Polygon	6.8°E–8.4°E	123°W–120.5°W	138.95°E–139.35°E	
	45.9°N–46.65°N	36.0°N–39.0°N	34.08°N–35.05°N	
M_c (EMR)	1.5 ± 0.13	1.20 ± 0.07	1.25 ± 0.05	5.39 ± 0.04
b (EMR)	0.96 ± 0.07	0.98 ± 0.02	0.81 ± 0.02	0.89 ± 0.01
M_c (MAXC)	1.36 ± 0.07	1.2 ± 0.00	1.2 ± 0.00	5.31 ± 0.03
M_c (GFT90)	1.31 ± 0.07	1.07 ± 0.04	1.07 ± 0.04	5.30 ± 0.00
M_c (GFT95)	1.58 ± 0.12	1.12 ± 0.04	1.12 ± 0.04	Not determined
M_c (MBS)	1.64 ± 0.11	1.44 ± 0.12	1.44 ± 0.12	5.94 ± 0.34

*Swiss Seismological Service.
†Northern California Seismic Network.
‡National Research Institute for Earth Science and Disaster Prevention.
§Harvard Centroid Moment Tensor.

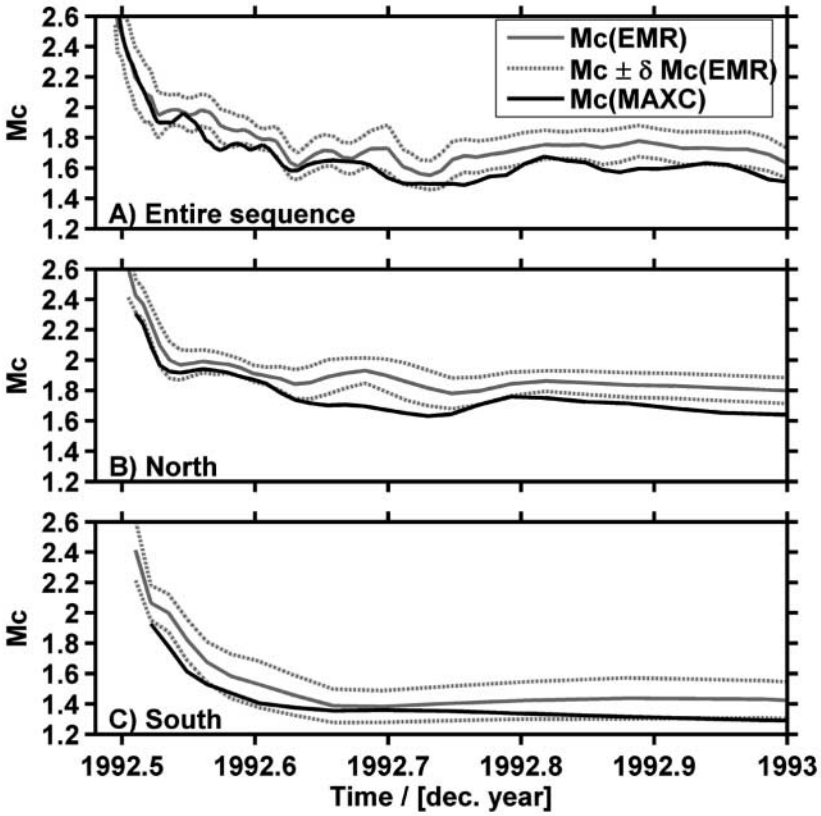

Figure 7. M_c as a function of time for (A) the entire 1992 Landers aftershock sequence, (B) the northernmost (20 km) aftershocks of the rupture zone, and (C) the southernmost (20 km) aftershocks. M_c(EMR) and δM_c(EMR) are plotted as gray lines; results of the MAXC approach as black lines. M_c for the entire sequence shows average values compared to the results obtained for limited regions.

differentiation of tectonic provinces is implicitly included when mapping M_c on an equally spaced grid ($2^\circ \times 2^\circ$).

The Harvard CMT catalogue for the period 1983–2002 in the depth range $d \leq 70$ km contains a total of about 12,650 events. We use a constant radius of $R = 1000$ km to create sub-catalogues at each grid node, and $N_{Bst} = 200$ bootstrap samples to calculate uncertainties. We require $N_{min} = 60$ events per node due to the sparse dataset. About 60% of the nodes have sample sizes between $60 \leq N \leq 150$ events. The magnitude ranges ΔM for single nodes vary in between 1 and 3. The ISC catalogue in the period 1983–2000 ($M \geq 4.3$) contains about 83,000 events. As more data is available, we chose $R = 900$ km, $N_{Bst} = 200$, $N_{min} = 60$. Here, only about 5% of the grid nodes have fewer than $N = 150$ events; the magnitude ranges also vary between 1 and 3. We admit that the choice of parameters for the Harvard CMT catalogue is at a very low margin, but for coverage purposes a larger N_{min} is not suitable. The smaller amount of data reduces the capabilities to obtain a good fit in the magnitude range below the magnitude of completeness.

M_c(EMR) varies for the Harvard CMT catalogue in general around M_c 5.6 (Fig. 8A). The lowest values of approximately $5.3 \leq M_c \leq 5.5$ are observed spanning the circum-Pacific region from Alaska and the Aleutians down to New Zealand and to the islands of Java and Indonesia. The west coasts of North and South America show slightly higher M_c-values (M_c 5.5–5.7) with larger fluctuations. Uncertainties δM_c are small ($\delta M_c \leq 0.15$) generally, as a consequence of sufficiently large datasets or peaked non-cumulative frequency-magnitude distributions (Fig. 8B). The highest values of about $M_c \geq 5.8$ are obtained in the two red regions close to Antarctica probably due to sparse data ($N \leq 100$) as a consequence of poor network coverage, a small magnitude range of about $\Delta M = 1.2$, and a flat distribution of the non-cumulative frequency of magnitudes. These results correlate well with the larger uncertainty of $\delta M_c \geq 0.2$. The Mid-Atlantic ridge is covered only between 25° N and S latitude, with M_c values primarily below 5.6.

The ISC catalogue shows in general a lower completeness in levels than does the Harvard CMT catalogue. In continental regions, M_c varies between 4.3 and 4.5, whereas on the Atlantic ridges values fluctuate between 4.6 and 5.1 (Fig. 8C). Uncertainties in δM_c display the same picture with values of $\delta M_c \leq 0.11$ in continental regions and higher values ($0.12 \leq \delta M_c \leq 0.35$) on Atlantic ridges and, especially, in the South Pacific near Antarctica (Fig. 8D). As the ISC is a combination of different catalogues, magnitudes had to be converted to be comparable, and this might be the reason for larger uncertainties in some regions.

Two examples from different tectonic regimes for regions in South America (subduction/spreading riged) and Japan (subduction) illustrate aspects of the relation between FMDs, M_c, and δM_c respectively, in Figure 9. Gray circles in Figure 8A show the respective locations. In case of Figure 9A the relatively flat frequency-magnitude distribution and small sample size ($N \approx 180$) for the South American ex-

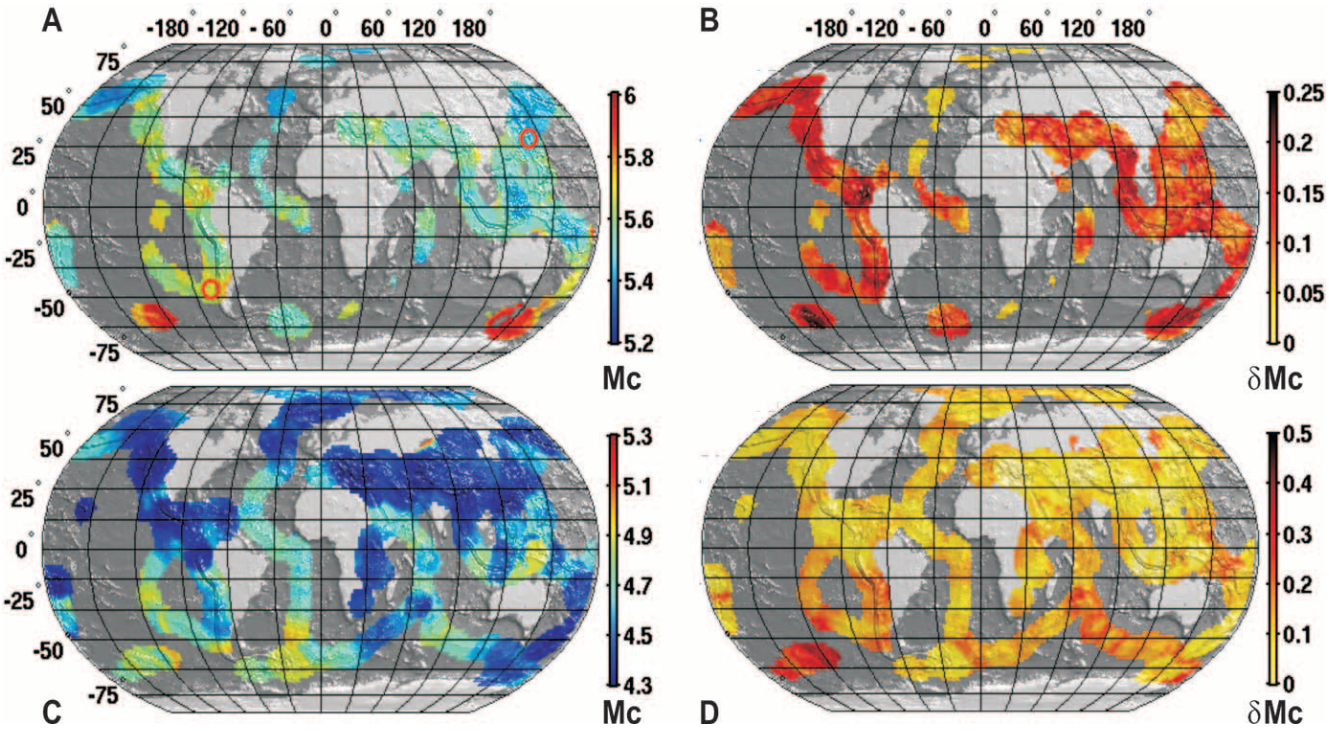

Figure 8. Global maps of M_c. Panels A and B illustrate M_c and δM_c using the Harvard CMT catalogue 1983–2002 for seismicity in the depth range $d \leq 70$ km, and constant radii R = 1000 km. The red circles indicate the spots for which frequency-magnitude distributions are shown in Figure 9. Panels C and D display M_c and δM_c of the ISC catalogue ($M \geq 4$) for the time period 1980–2001 ($d \leq 70$ km, R = 900 km). M_c-values are calculated as the mean of $N = 200$ bootstrap samples using the EMR method for the Harvard CMT catalogue and the MAXC method for the ISC.

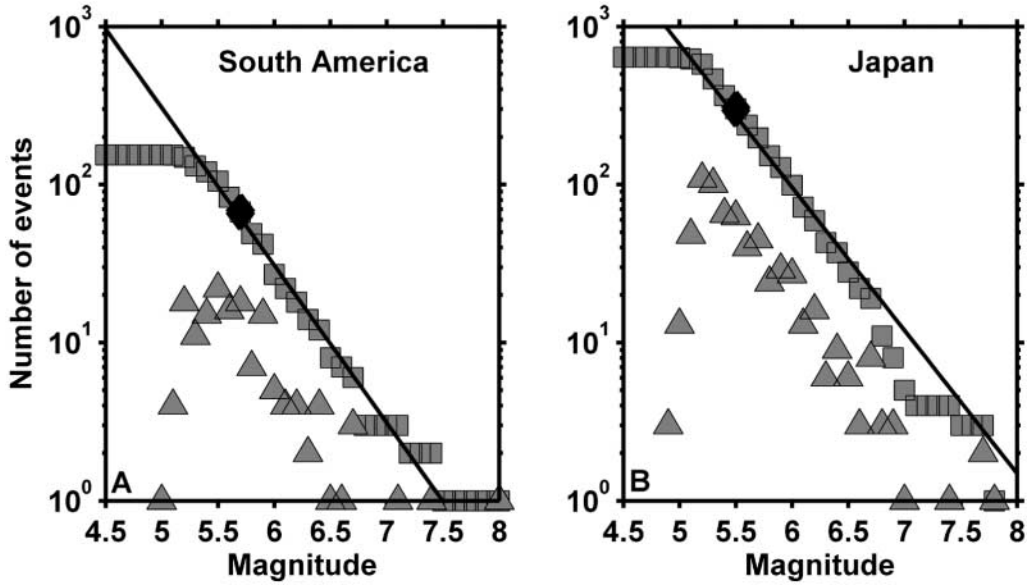

Figure 9. Cumulative and non-cumulative frequency-magnitude distributions from grid nodes indicated as red circles in Figure 8A: (A) South America (subduction/ridge): a flat frequency-magnitude distribution leading to relatively high uncertainties, M_c(EMR) = 5.7 ± 0.15; (B) Japan: a peaked frequency-magnitude distribution resulting in small uncertainties, M_c(EMR) = 5.5 ± 0.06.

ample leads to relatively high uncertainties in M_c 5.68 $\pm$ 0.15 (Fig. 9A). A small uncertainty is found for the peaked distribution in Figure 9B (Japan) where the small uncertainties M_c 5.47 $\pm$ 0.06 are also expected due to the large sample size.

Discussion

Finding the Best Approach to Determining M_c

We introduced the EMR method based on Ogata and Katsura (1993) to model the entire frequency-magnitude distribution with two functions: a normal cumulative distribution function and a Gutenberg-Richter power-law. M_c is based on maximum-likelihood estimates. The choice of the normal cumulative distribution function is based on visual inspection and modeling of a variety of catalogues, as well as comparisons to other possible functions, but is not based on physical reasoning. Thus, cases exist for which the choice of another function might be more appropriate. However, synthetic tests endorse that estimates of M_c can be correct even if this assumption is violated (Fig. 4).

Compared to other methods, the EMR method maximizes the amount of data available for the M_c determination, which should serve to stabilize the M_c estimates; however, it also adds two additional free parameters. Results from our synthetic test (Figs. 4 and 5) and case studies (Figs. 6, 7, 8) confirm that M_c(EMR), together with the bootstrap approach, performs best of all methods investigated for automatic mapping, justifying the additional free parameters. From these results we believe that the EMR method is indeed well capable of resolving M_c. It also has the additional benefit of delivering a complete seismicity model, which may be used in search for M_c changes, magnitude shifts, or rate changes. However, the EMR method is time consuming compared to MAXC, which is especially important when mapping large regions with large numbers of bootstrap samples. Additionally, the approach should only be applied when the incomplete part of the catalogues is available. Kagan (2002) argued that the normal CDF, acting as a thinning function on the Gutenberg-Richter law, may distort conclusions, as the smaller earthquakes may not have statistical stability. We instead believe that using the algorithm we provide minimizes the risk of questionable interpretations, especially because the fitting quality can be tested for using the KS test.

Cao and Gao (2002) published a method based on the assumption that *b*-values stabilize above the magnitude of completeness (Figs. 3C and D). We enhanced this approach by adding a criterion based on the *b*-value uncertainty to decide on the threshold, and by adding a smoothing window to ensure robust automatic fits. However, our synthetic tests showed that M_c(MBS) depends strongly on the sample size (Fig. 5B), and uncertainties are larger compared to other methods due to the linearity of the FMD. We found the method applicable only for regional catalogues. Note that the resulting M_c(MBS) is always higher than other M_c estimates (Fig. 6). In summary, we conclude that M_c(MBS) cannot be used for automatic determination of M_c(MBS), but spot-checking *b* as a function of the cutoff magnitude M_{co} (Fig. 3) can give important clues about M_c and *b*.

The MAXC approach and the GFT approach (Wiemer and Wyss, 2002) tend to underestimate the magnitude of completeness. This is found in our synthetic catalogue analysis (Fig. 5), confirmed in the analysis of various catalogues (Fig. 6) and for the case study of the Landers aftershock sequence (Fig. 7). The advantage of M_c(MAXC) is that results can be obtained with low computational effort for small sample sizes and in pre-cut catalogues. M_c(GFT), on the other hand, shows a smaller systematic bias; however, it is slightly more computational intensive and not robust for small sample sizes $S < 200$.

The application of the EMR and MAXC approaches to the 1992 Landers aftershock sequence shows that M_c was slightly underestimated by 0.2 in Wiemer and Katsumata (1999) (Fig. 7). The reevaluation displays the importance of the spatial and temporal assessment of M_c, as it has proven to be a crucial parameter in a variety of studies, especially when working on real-time time-dependent hazard estimates for daily forecasts (Gerstenberger, 2003).

We applied a gridding technique rather than assuming predefined Flinn-Engdahl regions (Frohlich and Davis, 1993; Kagan, 1999) to map M_c for global catalogues (Fig. 8). The maps reveal considerable spatial variations in M_c on a global scale in both the Harvard CMT ($5.3 \leq M_c \leq 6.0$) and ISC catalogue ($4.3 \leq M_c \leq 5.0$).

The overall M_c values we compute, for example, for the entire Harvard catalog (M_c 5.4; Fig. 6) are often lower than the maximum value found when mapping out M_c in space and/or time. Technically, one might argue that the overall completeness cannot be lower than any of its subsets. Given that in the seconds and minutes after a large mainshock, such as Landers, even magnitude 6 events may not be detectable in the coda of the mainshock; for practical purposes, completeness is best not treated in this purist view, since 100% completeness can never be established. The contribution of the relatively minor incomplete subsets, such as the regions with high M_c in the southern hemisphere (Fig. 8) are generally not relevant when analyzing the overall behavior of the catalogue. Such subsets, however, need to be identified when analyzing spatial and temporal variations of seismicity parameters, thus highlighting the importance of the presented quantitative techniques to map M_c.

Conclusion

We demonstrated that the EMR method is the most favorable choice to determine M_c (1) because the method is stable under most conditions; (2) because a comprehensive seismicity model is computed; and (3) because the model fit can be tested. We conclude that:

- for automated mapping purposes, the mean value of the N bootstrapped M_c determinations is a suitable estimate of M_c because it avoids outliers and smoothes the results;
- the bootstrap approach to determine uncertainties in M_c is a reliable method;
- for a fast analysis of M_c, we recommend using the MAXC approach in combination with the bootstrap and add a correction value (e.g., $M_c = M_c(\text{MAXC}) + 0.2$). This correction factor can be determined by spot-checking individual regions and is justified by the analysis of the synthetic catalogues.

Acknowledgments

The authors would like to thank D. Schorlemmer, M. Mai, M. Wyss, and J. Hauser for helpful comments to improve the manuscript and programming support. We are indebted to the associate editor J. Hardebeck and three anonymous reviewers for valuable comments that significantly enhanced the manuscript. We acknowledge the Northern and Southern Earthquake Data Centers for distributing the catalogues of the Northern California Seismic Network (NCSN) and the Southern California Seismic Network (SCSN), and the Japanese Meterological Agency (JMA), the Swiss Seismological Service, the International Seismological Center and the Harvard Seismology Group for providing seismicity catalogues used in this study. Figure 1 was created using Generic Mapping Tools (GMT) (Wessel and Smith, 1991). This is contribution number 1372 of the Institute of Geophysics, ETH Zurich.

References

Abercrombie, R. E., and J. N. Brune (1994). Evidence for a constant *b*-value above magnitude 0 in the southern San Andreas, San Jacinto, and San Miguel fault zones and at the Long Valley caldera, California, *Geophys. Res. Lett.* **21,** 1647–1650.

Aki, K. (1965). Maximum likelihood estimate of b in the formula $\log N = a - bM$ and its confidence limits, *Bull. Earthq. Res. Inst. Tokyo Univ.* **43,** 237–239.

Albarello, D., R. Camassi, and A. Rebez (2001). Detection of space and time heterogeneity in the completeness of a seismic catalog by a statistical approach: An application to the Italian area, *Bull. Seism. Soc. Am.* **91,** 1694–1703.

Bender, B. (1983). Maximum likelihood estimation of *b*-values for magnitude grouped data, *Bull. Seism. Soc. Am.* **73,** 831–851.

Cao, A. M., and S. S. Gao (2002). Temporal variation of seismic *b*-values beneath northeastern Japan island arc, *Geophys. Res. Lett.* **29,** no. 9, doi 10.1029/2001GL013775.

Chernick, M. R. (1999). Bootstrap methods: A practitioner's guide, in *Wiley Series in Probability and Statistics*, W. A. Shewhart (Editor), Wiley and Sons, Inc., New York.

Conover, W. J. (1999). *Applied Probability and Statistics* Third Ed. Wiley and Sons Inc., New York.

Deichmann, N., M. Baer, J. Braunmiller, D. B. Dolfin, F. Bay, F. Bernardi, B. Delouis, D. Faeh, M. Gerstenberger, D. Giardini, S. Huber, U. Kradolfer, S. Maraini, I. Oprsal, R. Schibler, T. Schler, S. Sellami, S. Steimen, S. Wiemer, J. Woessner, and A. Wyss (2002). Earthquakes in Switzerland and surrounding regions during 2001, *Eclogae Geologicae Helvetiae* **95,** 249–262.

Dziewonski, A. M., G. Ekstrom, and N. N. Maternovskaya (1999). Centroid-moment tensor solutions for October–December, 1998. *Phys. Earth Planet. Inter.* **115,** 1–16.

Efron, B. (1979). 1977 Rietz Lecture, Bootstrap Methods—Another Look at the Jackknife, Ann. Statist. **7,** 1–26.

Enescu, B., and K. Ito (2002). Spatial analysis of the frequency-magnitude distribution and decay rate of aftershock activity of the 2000 Western Tottori earthquake, *Earth Planet Space* **54,** 847–859.

Faeh, D., D. Giardini, F. Bay, M. Baer, F. Bernardi, J. Braunmiller, N. Deichmann, M. Furrer, L. Gantner, M. Gisler, D. Isenegger, M. J. Jimenez, P. Kaestli, R. Koglin, V. Masciadri, M. Rutz, C. Scheidegger, R. Schibler, D. Schorlemmer, G. Schwarz-Zanctti, S. Steimen, S. Sellami, S. Wiemer, and J. Woessner (2003). Earthquake Catalog Of Switzerland (ECOS) and the related macroseismic database, *Eclogae Geologicae Helvetiae* **96,** 219–236.

Frohlich, C., and S. Davis (1993). Teleseismic *b*-values: or much ado about 1.0. *J. Geophys. Res.* **98,** 631–644.

Gerstenberger, M., S. Wiemer, and D. Giardini (2001). A systematic test of the hypothesis that the *b* value varies with depth in California, *Geophys. Res. Lett.* **28,** no. 1, 57–60.

Gerstenberger, M. C. (2003). Earthquake clustering and time-dependent probabilistic seismic hazard analysis for California, in *Institute of Geophysics*, Swiss Fed. Inst. Tech., Zurich, 180 pp.

Gomberg, J. (1991). Seismicity and detection/location threshold in the southern Great Basin seismic network, *J. Geophys. Res.* **96,** 16,401–16,414.

Gomberg, J., P. Reasenberg, P. Bodin, and R. Harris (2001). Earthquake triggering by seismic waves following the Landers and Hector Mine earthquakes, *Nature* **411,** 462–466.

Gutenberg, R., and C. F. Richter (1944). Frequency of earthquakes in California. *Bull. Seism. Soc. Am.* **34,** 185–188.

Habermann, R. E. (1987). Man-made changes of seismicity rates. *Bull. Seism. Soc. Am.* **77,** 141–159.

Habermann, R. E. (1991). Seismicity rate variations and systematic changes in magnitudes in teleseismic catalogs, *Tectonophysics* **193,** 277–289.

Habermann, R. E., and F. Creamer (1994). Catalog errors and the M8 earthquake prediction algorithm, *Bull. Seism. Soc. Am.* **84,** 1551–1559.

Ide, S., and G. C. Beroza (2001). Does apparent stress vary with earthquake size? *Geophys. Res. Lett.* **28,** no. 17, 3349–3352.

Ishimoto, M., and K. Iida (1939). Observations of earthquakes registered with the microseismograph constructed recently, *Bull. Earthq. Res. Inst.* **17,** 443–478.

Kagan, Y. Y. (1999). Universality of the seismic moment-frequency relation, *Pure Appl. Geophys.* **155,** 537–574.

Kagan, Y. Y. (2002). Seismic moment distribution revisited: I. Statistical results, *Geophys. J. Int.* **148,** 520–541.

Kagan, Y. Y. (2003). Accuracy of modern global earthquake catalogs, *Phys. Earth Planet. Inter.* **135,** 173–209.

Knopoff, L. (2000). The magnitude distribution of declustered earthquakes in Southern California, Proc. Nat. Acad. Sci. **97,** 11,880–11,884.

Kvaerna, T., F. Ringdal, J. Schweitzer, and L. Taylor (2002a). Optimized seismic threshold monitoring—Part 1: Regional processing, *Pure Appl. Geophys.* **159,** 969–987.

Kvaerna, T., F. Ringdal, J. Schweitzer, and L. Taylor (2002b). Optimized seismic threshold monitoring—Part 2: Teleseismic processing, *Pure Appl. Geophys.* **159,** 989–1004.

Liu, J., K. Sieh, and E. Hauksson (2003). A structural interpretation of the aftershock "Cloud" of the 1992 M_w 7.3 Landers earthquake, *Bull. Seism. Soc. Am.* **93,** 1333–1344.

Main, I. (2000). Apparent breaks in scaling in the earthquake cumulative frequency-magnitude distribution: fact or artifact? *Bull. Seism. Soc. Am.* **90,** 86–97.

Marsan, D. (2003). Triggering of seismicity at short timescales following Californian earthquakes, *J. Geophys. Res.* **108,** no. B5, 2266, doi 10.1029/2002JB001946.

Ogata, Y., and K. Katsura (1993). Analysis of temporal and spatial heterogeneity of magnitude frequency distribution inferred from earthquake catalogs, *Geophys. J. Int.* **113,** 727–738.

Ogata, Y., L. M. Jones, and S. Toda (2003). When and where the aftershock activity was depressed: contrasting decay patterns of the proximate

large eathquakes in Southern California, *J. Geophys. Res.* **108,** no. B6, doi 10.1029/2002JB002009.

Rydelek, P. A., and I. S. Sacks (1989). Testing the completeness of earthquake catalogs and the hypothesis of self-similarity, *Nature* **337,** 251–253.

Rydelek, P. A., and I. S. Sacks (2003). Comment on "Minimum magnitude of completeness in earthquake catalogs: examples from Alaska, the Western United States, and Japan" by Stefan Wiemer and Max Wyss, *Bull. Seism. Soc. Am.* **93,** 1862–1867.

Schorlemmer, D., G. Neri, S. Wiemer, and A. Mostaccio (2003). Stability and significance tests for *b*-value anomalies: examples from the Tyrrhenian Sea, *Geophys. Res. Lett.* **30,** no. 16, 1835, doi 10.1029/2003GL017335.

Shi, Y., and B. A. Bolt (1982). The standard error of the magnitude-frequency *b*-value, *Bull. Seism. Soc. Am.* **72,** 1677–1687.

Stein, R. S. (1999). The role of stress transfer in earthquake occurrence, *Nature* **402,** 605–609.

Taylor, D. W. A., J. A. Snoke, I. S. Sacks, and T. Takanami (1990). Nonlinear frequency-magnitude relationship for the Hokkaido corner, Japan, *Bull. Seism. Soc. Am.* **80,** 340–353.

Utsu, T. (1965). A method for determining the value of *b* in a formula log $n = a - bM$ showing the magnitude frequency for earthquakes, *Geophys. Bull. Hokkaido Univ.* **13,** 99–103.

Utsu, T. (1999). Representation and analysis of the earthquake size distribution: a historical review and some new approaches, *Pageoph* **155,** 509–535.

Von Seggern, D. H., J. N. Brune, K. D. Smith, and A. Aburto (2003). Linearity of the earthquake recurrence curve to $M < -1$ from Little Skull Mountain aftershocks in Southern Nevada, *Bull. Seism. Soc. Am.* **93,** 2493–2501.

Wessel, P., and W. H. F. Smith (1991). Free software helps map and display data, *EOS Trans. AGU* **72,** 441, 445–446.

Wiemer, S. (2000). Introducing probabilistic aftershock hazard mapping, *Geophys. Res. Lett.* **27,** 3405–3408.

Wiemer, S. (2001). A software package to analyze seismicity: ZMAP, *Seism. Res. Lett.* **72,** 373–382.

Wiemer, S., and K. Katsumata (1999). Spatial variability of seismicity parameters in aftershock zones, *J. Geophys. Res.* **104,** 13,135–13,151.

Wiemer, S., and M. Wyss (1994). Seismic quiescence before the Landers (*M* 7.5) and Big Bear (*M* 6.5) 1992 earthquakes, *Bull. Seism. Soc. Am.* **84,** 900–916.

Wiemer, S., and M. Wyss (2000). Minimum magnitude of complete reporting in earthquake catalogs: examples from Alaska, the Western United States, and Japan, *Bull. Seism. Soc. Am.* **90,** 859–869.

Wiemer, S., and M. Wyss (2002). Mapping spatial variability of the frequency-magnitude distribution of earthquakes, *Adv. Geophys.* **45,** 259–302.

Wiemer, S., and M. Wyss (2003). Reply to "Comment on 'Minimum magnitude of completeness in earthquake catalogs: examples from Alaska, the Western United States and Japan' by Stefan Wiemer and Max Wyss," *Bull. Seism. Soc. Am.* **93,** 1868–1871.

Woessner, J., E. Hauksson, S. Wiemer, and S. Neukomm (2004). The 1997 Kagoshima (Japan) earthquake doublet: a quantitative analysis of aftershock rate changes, *Geophys. Res. Lett.* **31,** L03605, doi 10.1029/2003/GL018858.

Wyss, M., and S. Wiemer (2000). Change in the probability for earthquakes in Southern California due to the Landers magnitude 7.3 earthquake, *Science* **290,** 1334–1338.

Zuniga, F. R., and S. Wiemer (1999). Seismicity patterns: are they always related to natural causes? *Pure Appl. Geophys.* **155,** 713–726.

Institute of Geophysics
ETH Hönggerberg
CH-8093
Zürich, Switzerland
jochen.woessner@sed.ethz.ch
(J.W.)

Manuscript received 12 January 2004.